Mapping the Energy of Superantigen *Staphylococcus* Enterotoxin C3 Recognition of an α/β T Cell Receptor Using Alanine Scanning Mutagenesis

By Hywyn R.O. Churchill,* Peter S. Andersen,‡ Evan A. Parke,*
Roy A. Mariuzza,‡ and David M. Kranz*

*From the *Department of Biochemistry, University of Illinois, Urbana, Illinois 61801; and the
‡Center for Advanced Research in Biotechnology, University of Maryland Biotechnology Institute,
Rockville, Maryland 20850*

Abstract

Binding of the T cell receptor (TCR) to a bacterial superantigen (SAG) results in stimulation of a large population of T cells and subsequent inflammatory reactions. To define the functional contribution of TCR residues to SAG recognition, binding by 24 single-site alanine substitutions in the TCR Vβ domain to *Staphylococcus aureus* enterotoxin (SE) C3 was measured, producing an energy map of the TCR–SAG interaction. The results showed that complementarity determining region 2 (CDR2) of the Vβ contributed the majority of binding energy, whereas hypervariable region 4 (HV4) and framework region 3 (FR3) contributed a minimal amount of energy. The crystal structure of the Vβ8.2–SEC3 complex suggests that the CDR2 mutations act by disrupting Vβ main chain interactions with SEC3, perhaps by affecting the conformation of CDR2. The finding that single Vβ side chain substitutions had significant effects on binding and that other SEC3-reactive Vβ are diverse at these same positions indicates that SEC3 binds to other TCRs through compensatory mechanisms. Thus, there appears to be strong selective pressure on SAGs to maintain binding to diverse T cells.

Key words: T cell receptor • superantigens • *Staphylococcus aureus* • T cell recognition • septic shock

Introduction

A T cell recognizes ligand through the interaction of its α/β TCR and an antigenic peptide expressed in the context of an MHC (pMHC). This process of MHC restriction provides for the specificity of T cell responses to pathogens. Superantigens (SAGs)[1] are proteins of viral or bacterial origin that stimulate T cell populations by binding and cross-linking the TCR with a class II MHC product, thus circumventing the normal recognition of intracellularly processed pMHC (1). Because SAGs can bind to Vβ regions directly, SAG engagement of T cells leads to polyclonal expansion of up to 20% of all T cells. In contrast, normal pMHC antigen recognition might involve the stimulation of as few as only 1 in 10^5 or 10^6 T cells (2). SAG-mediated recognition can lead to hyperactive responses associated with the release of T cell cytokines or to T cell deletion and anergy (3, 4). It has also been suggested that SAG-mediated effects may contribute to particular autoimmune and inflammatory disorders (3).

Two classes of SAGs have been identified: endogenous retroviral-encoded cellular-bound proteins, such as mouse mammary tumor virus (MMTV)-encoded Mls antigen, and exogenous soluble proteins secreted from bacteria (4–6). The latter SAGs include *Mycoplasma arthritidis* mitogen (7, 8), streptococcal pyrogenic exotoxins (9–11), staphylococcal toxic shock syndrome toxin 1, enterotoxins, and exfoliative toxins (1, 9). Most structural and biological activity studies have focused on the SAGs of *Staphylococcus aureus*, which have been associated with food poisoning and toxic shock syndrome (3).

The *S. aureus* enterotoxins (SEs) exist in isoforms A–E and G–I (12), which bind to numerous Vβ families of murine and human origin (1). The structures of SEs to date reveal a conserved architecture, consisting of a small NH_2-terminal

β-barrel domain and a large COOH-terminal domain that contains a β-grasp motif, connected by a long solvent-accessible α helix (2). Early studies suggested that the SE-binding site of the TCR was positioned away from the conventional pMHC combining site (13). The Vβ cross-reactivity possessed by SEs suggested that the proteins bound to conserved structural elements of the TCR shared among different Vβ regions (1). Mutagenesis studies indicated that CDR2, and perhaps CDR1 to a lesser degree, were involved in the reactivity with SEB and SEA (14).

The recent crystallographic structures of SEC3 and SEB in complex with the Vβ8.2 region of the mouse TCR 14.3.d (15, 16) revealed that CDR2, hypervariable region 4 (HV4), and framework region 3 (FR3) contact these SAGs. In both complexes, CDR2 occupied the cleft between the large and small domains of SEC3 and shared multiple contacts and hydrogen bonds with each domain (17). CDR2 contained the majority of surface contacts for SEC3 (63%) and for SEB (50%), and these contacts involved exclusively Vβ main chain atoms. The FR3 region of the Vβ domain contributed 32 and 34% of the contacts with SEC3 and SEB, whereas HV4 provided 7 and 9% of the contacts with SEC3 and SEB (16). Direct contacts with CDR1 and CDR3 were not observed in either complex. Therefore, SE binding to the TCR incorporates regions of the TCR that are essential in pMHC binding (CDR2), while also involving regions that are not important in pMHC recognition (FR3 and HV4).

SAGs stimulate T cells not just by binding to the TCR, but by binding a class II MHC product through a different face of the SAG molecule. This TCR–SAG–pMHC ternary complex brings a T cell together with a class II$^+$ cell and it presumably leads to TCR clustering at the T cell surface. The stoichiometry of these interactions has yet to be fully determined and may vary among the different SAGs (12). Nevertheless, recent evidence showed that the Vα of the TCR appears to be involved in binding to the class II MHC product and thereby increasing the stability of the complexes (18). This finding is consistent with the initial work of Blackman and colleagues and more recently from other groups that suggested that SAG-mediated effects may involve CDR3 of the β chain and the Vα region (8, 19–25). The latter conclusions were based on evidence of restrictions in either CDR3 residues or Vα regions that were expressed by a specific Vβ$^+$ population that reacted with an SAG.

Although the structure of individual components and the complexes have provided a view of the contact residues, mutagenesis studies can provide a quantitative view of the residues that are of importance from the energetic perspective. These interactions usually represent a subset of the interface residues identified as contacts in the crystal structure (26). However, even the same protein surface can involve either only a few very important residues in ligand binding (e.g., the antibody D1.3 in its interaction with hen egg lysozyme) or a larger number of moderately important residues (e.g., the D1.3 interaction with its antiidiotype antibody E5.2) (27). This possibility is important with regard to Vβ–SEC3 interactions, as it is possible that the majority of the energy could be derived from only a few contacts and

these contacts might be conserved among the different SEC3-reactive Vβ regions.

To define the functional contribution of individual TCR residues toward SEC3 recognition, we have used alanine scanning mutagenesis of a Vβ8.2 TCR from the T cell clone 2C. Due to the relatively low affinity of the SEC3–Vβ8.2 TCR interaction (equilibrium binding constant [K_D] > 10 μM), an affinity-matured SEC3 variant (K_D ∼ 180 nM) was used to facilitate the mutagenic binding studies. Residues in CDR1 and CDR2, and to a lesser degree HV4 and FR3, served as energetic hotspots for binding to the SEC3 variant. Based on the structure of the Vβ8–SEC3 complex (16), most of the CDR1 energy was predicted to be involved in binding the region of the SEC3 variant that had been mutated to yield higher affinity. Thus, CDR2 contributed the majority of the energy to the interaction of Vβ8.2 and the wild-type (wt) SEC3. HV4 and FR3 contributed less energy than would be predicted from their contribution to the total contact area of the complex. The observation that CDR2 mutations affected binding to SEC3 is somewhat surprising in the sense that all of the contacts found at the CDR2–SEC3 interface involved Vβ main chain interactions (16). Side chain substitutions could be affecting these main chain interactions through conformational changes in the Vβ8 backbone.

As other Vβ regions that interact with SEC3 exhibit even more amino acid variability at the energetically important positions (i.e., than a single alanine mutation), there appears to be extensive diversity at the molecular level in the binding of SEC3 to different Vβ regions. Thus, from a consideration of binding energies the results provide evidence that the same SAG may require compensatory interactions among different Vβ regions. These interactions could involve other residues within the Vβ (i.e., residues different from those important in the Vβ8.2–SEC3 interaction) or residues within CDR3 loops or Vα regions that act by contacting and stabilizing the interaction with class II MHC. In light of the minimal binding energy differences that are known to elicit agonist versus antagonist responses (28, 29), the results also suggest how the same SAG could yield widely disparate biological affects, depending on the Vβ region involved.

Materials and Methods

TCR Mutagenesis. Alanine-substituted single-chain (sc)TCRs were constructed as thioredoxin fusion proteins with a His$_6$ tag using two mutagenesis methods. First, a PCR-based technique (30) used a short mutagenic primer and a Vβ-specific primer to generate a "megaprimer," which was isolated and used in a second PCR with the opposing Vα-specific primer. All PCRs were carried out using cloned *Pfu* DNA polymerase (Stratagene). The KpnI/BamHI-digested PCR product was ligated into a pUC-19M vector, transformed into *Escherichia coli* strain DH5-α for sequencing. The scTCR inserts were then subcloned into the pTRXFus vector (Invitrogen) and transformed into *E. coli* strain GI698 for expression. Alternatively, "QuikChange" site-directed mutagenesis (Stratagene) was used to mutagenize the wt-scTCR-pTRXFus. The DpnI-digested product was transformed into *E. coli* strain GI698 for sequencing and expression.

TCR Expression and Purification. Proteins were expressed in *E. coli* strain GI698 as described previously (31) and purified from inclusion bodies by denaturing affinity chromatography using His-Bind resin (Novagen). After renaturation by dialysis (31), the monomeric proteins were purified by Superdex 200 gel filtration (Amersham Pharmacia Biotech) using HPLC.

mAbs. KJ16 (32) is a rat IgG mAb specific for mouse Vβ8.1 and Vβ8.2 regions of the TCR. F23.1 (33) is a mouse IgG2a mAb specific for mouse Vβ8.1, Vβ8.2, and Vβ8.3 regions. F23.2 (33) is a mouse IgG1 mAb specific for the mouse Vβ8.2 region. Antibodies were purified from either culture supernatants or ascites, followed by protein G– and protein A–agarose (GIBCO BRL) column chromatography for KJ16 and F23.1/F23.2, respectively.

SEC3 Purification. SEC3 variant 1A4 (SEC3-1A4) was isolated from a phage display library (Anderson, P.S., and R.A. Mariuzza, manuscript in preparation). Soluble protein was prepared as described previously (18). In brief, bacterial expression was induced at mid-log density by the addition of isopropyl-β-d-thiogalactopyranoside (IPTG) and continued for 4 h. The protein was purified from the periplasmic fraction using a RedA dye–agarose matrix (Amicon), followed by chromatography using a monoQ column (Amersham Pharmacia Biotech).

ELISAs. Vβ8–specific competition ELISAs were performed by adsorption of KJ16, F23.1, or F23.2 to the wells of Immulon 2HB analytical plates (Dynatech Labs). The wells were blocked with PBS that contained 0.25% BSA and 0.05% Tween 20. After washing, 100 μl of mutant or wt-scTCR and 50 μl of biotinylated wt-scTCR were added to the wells for 1 h The wells were then washed, and binding was detected using horseradish peroxidase (HRP)-streptavidin followed by tetramethylbenzidine (TMB) peroxidase substrate (Kirkegaard & Perry). The relative half-maximal inhibitory concentration (IC_{50}) for each mutant relative to wt was calculated using linear regression analysis.

SEC3-1A4 competition ELISAs were performed by adsorption of wt-scTCR to the wells of the analytical plates. The wells were blocked and after washing, 50 μl of mutant or wt-scTCR and 50 μl of biotinylated SEC3-1A4 were added to the wells. After 1 h, the wells were washed and binding was detected using HRP-streptavidin followed by TMB substrate. The relative IC_{50} for each mutant relative to wt was calculated using linear regression analysis. SEC3-1A4 reactivity was normalized for Vβ8 reactivity to account for variations in the percentages of properly folded scTCRs.

BIAcore Analysis. Surface plasmon resonance (SPR) studies were performed using a BIAcore 1000® instrument. Binding experiments were as described previously (17, 18). SEC3-1A4 was immobilized on the sensor chip, and various concentrations of scTCR were allowed to bind until equilibrium was reached (1–5 min). The response, corrected for nonspecific binding and aggregation (34), was used to determine the equilibrium binding constant (K_D) by Scatchard analysis.

Structural Analysis. Structural analysis was performed on an O_2 work station (Silicon Graphics) using Quanta 97 Software (Molecular Simulations). The structure of 14.3.d β chain–SEC3 complex (15), in conjunction with the structure of 2C TCR (35), was used to assign SEC3 contacts for those 2C residues tested by mutagenesis.

Results

Binding of 2C scTCR to SEC3 Wt and SEC3 Variant 1A4. The TCR used here is derived from the murine CTL clone 2C (36), which recognizes the allogeneic MHC L^d (37) and the syngeneic MHC K^b (38). The 2C TCR

contains the Vα3.1 region and the Vβ8.2 region. With the exception of CDR3β, this is the same Vβ expressed by the TCR 14.3.d that was crystallized as a complex with SEC3 (15). The 2C TCR was produced as a single chain containing an NH_2-terminal thioredoxin domain (for increased solubility), the Vβ region, a 24-residue linker, and the Vα region (31). The reactivity of the scTCR construct is similar to the native receptor for the allogeneic MHC ligand L^d (39, 40) and its syngeneic MHC ligand K^b (Lee, P.U.Y., H.R.O. Churchill, and D.M. Krantz, unpublished results).

The mAbs KJ16, F23.1, and F23.2 (32, 33) recognize conformational epitopes on the Vβ8 region (41). KJ16 and F23.1 react with framework regions (FRs) of the Vβ8 domain while F23.2 reacts with CDR1 and CDR2 residues (42). To develop a sensitive, quantitative binding assay for TCR mutants, we made use of an SEC3 variant, 1A4, that has a higher affinity for the TCR. This SEC3 variant was isolated by phage display of a library of SEC3 mutants, followed by selection on immobilized 14.3.d β chain (18). The SEC3 library contained random variants at five residues (102Gly, 103Lys, 104Val, 105Thr, and 106Gly) of the disulfide loop within the small domain of SEC3. Variant 1A4 and wt SEC3 were examined for binding to the 2C scTCR in a competition assay and in BIAcore analyses. The competition assay involved immobilization of F23.2 or KJ16 on wells, followed by addition of biotinylated scTCR and streptavidin-HRP. SEC3 wt and 1A4 were titrated as unlabeled inhibitors of this reaction (Fig. 1), showing that 1A4 was an ∼290-fold better inhibitor. Results were similar with either F23.2 or KJ16 as the immobilized antibody (data not shown).

SPR (BIAcore) analyses were performed using titrations of the 2C scTCR with either wt SEC3 or 1A4 immobilized on the surface of a chip (see below and Fig. 6). Based on equilibrium binding titrations, the wt 2C scTCR dis-
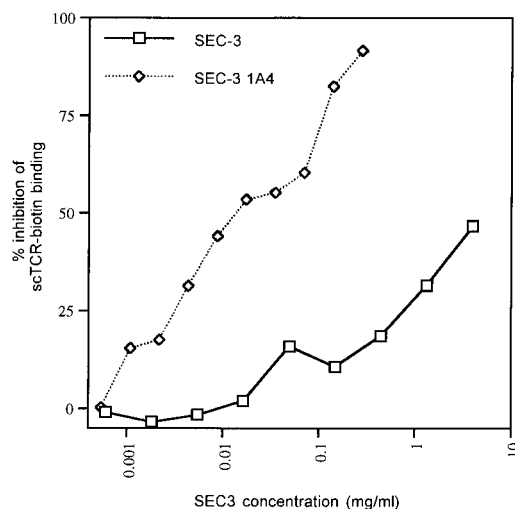

Figure 1. Relative TCR reactivities of SEC3 and SEC3 variant 1A4. Various concentrations of SEC3 wt and SEC3 variant 1A4 were used to inhibit binding of biotinylated scTCR to immobilized mAb KJ16 in an ELISA format. Bound biotinylated scTCR was detected by streptavidin-HRP. The relative reactivity of each SAG was determined as the ratio of SAG to scTCR IC_{50} by linear regression analysis. Similar results were obtained with immobilized mAb F23.2 (data not shown).

	CDR1								CDR2									FR3		HV4								CDR3							Vα3.1
Residue	25	26	27	28	29	30	31	32	48	49	50	51	52	53	54	55	56	57	66	69	70	71	72	73	74	75	76	95	96	97	98	105	106	107	100
Vβ8.2	Q	T	N	N	H	N	N	M	Y	S	Y	G	A	G	S	T	E	K	K	R	P	S	Q	E	N	F	S	G	G	G	G	T	L	Y	F
Mutant		*	*		*	*			*			*	W	*		*	*	*	*		*	*	*	*	*		*	*	*	*	*	*	*	*	*
Expression Defect	*				*			*		*					*					*						*									

Figure 2. 2C scTCR alanine substitutions and protein expression. Alanine mutants that can be expressed and properly refolded are indicated. Proteins listed as having an expression defect possessed minimal or no Vβ8-specific mAb activity by ELISA (see Fig. 3).

played a K_D of 180 ± 55 nM for the SEC3-1A4 variant, but the affinity for the wt SEC3 was not measurable ($K_D > 5 \, \mu M$) at the concentrations of scTCR that could be tested (i.e., the solubility limit of the 2C scTCR). Thus, the affinity of SEC3-1A4 was at least 30-fold higher based on this assay method. Similar results were obtained for binding of

Figure 3. Reactivity of scTCR alanine mutants with anti-Vβ8 antibodies. The relative reactivity of the mutant scTCR proteins toward the Vβ8-specific antibodies KJ16 (A) and F23.1 (B) were evaluated in a competition ELISA format. Various concentrations of wt and mutant scTCRs were used to inhibit the binding of biotinylated wt-scTCR to each antibody, followed by detection with streptavidin-HRP. The IC50 ratio of mutant to wt by linear regression analysis was used as a measure of antibody reactivity. The average value for each mutant was used as a normalization factor for properly refolded protein.

wt SEC3 and SEC3-1A4 variant to immobilized 14.3.d TCR-α/β yielding K_D values of 22 μM and 150 nM, respectively (data not shown). Together, these results showed that the SEC3-1A4 variant had sufficient affinity to perform a mutagenic analysis.

Characterization of 2C TCR Mutants. To analyze the interface between the TCR and SEC3-1A4, 29 single-site alanine mutants of the 2C scTCR (Fig. 2) were expressed in *E. coli* and purified by Ni column chromatography and gel filtration. As Vβ residue 52 is alanine, this position was mutated to tryptophan. The reactivities of the KJ16 and F23.1 antibodies with the mutant scTCR provided a measure of the concentration of folded protein in the preparations of refolded scTCR. Monomeric scTCR mutants were evaluated for Vβ-specific mAb reactivity in a competition ELISA using biotinylated wt-scTCR. The degree of properly folded scTCRs was determined from inhibition curves, as the IC50 relative to wt-scTCR (Fig. 3). The average reactivity of KJ16 and F23.1 with the scTCR was used as a measure of the concentration of properly folded protein.

23 of the single-site mutants showed reactivity with the anti-Vβ antibodies, KJ16 and F23.1, indicating that they were properly folded. Seven mutants (Vβ residues 25βGln, 29βHis, 32βMet, 49βSer, 54βSer, 69βArg, and 75βPhe) had minimal or no mAb reactivity. Most of these are inaccessible residues in which the side chains are likely to be involved in the stability of the CDR or HV4 loops (35). Mutations in the three CDRs and HV4 could be evaluated using KJ16 and F23.1, as these loops are not part of the KJ16 or F23.1 epitopes. Because mutations in the FRs 57βLys and 66βLys might affect binding to KJ16 and/or F23.1, mAb F23.2 was also used as verification of proper refolding of these mutants. The Lys57βAla and Lys66βAla mutants bound to F23.2, KJ16, and F23.1 with reactivities similar to the wt-scTCR, indicating that these residues do not contribute energy to the epitopes of any of these Vβ8-specific mAbs and that the mutants were properly refolded.

Binding of Single-Site TCR Mutants to SEC3-1A4. Binding affinities of the TCR mutants were also examined in two different assays. In one assay, an ELISA was performed with immobilized wt-scTCR followed by the addition of biotinylated SEC3-1A4 and streptavidin-HRP. The measurement of mutant scTCR affinities was evaluated by titrations with unlabeled scTCR to compete for SEC3 binding to the immobilized wt-scTCR. From the generation of binding inhibition curves (Fig. 4), the SEC3-1A4 reactivity was determined as the IC50 ratio of mutant
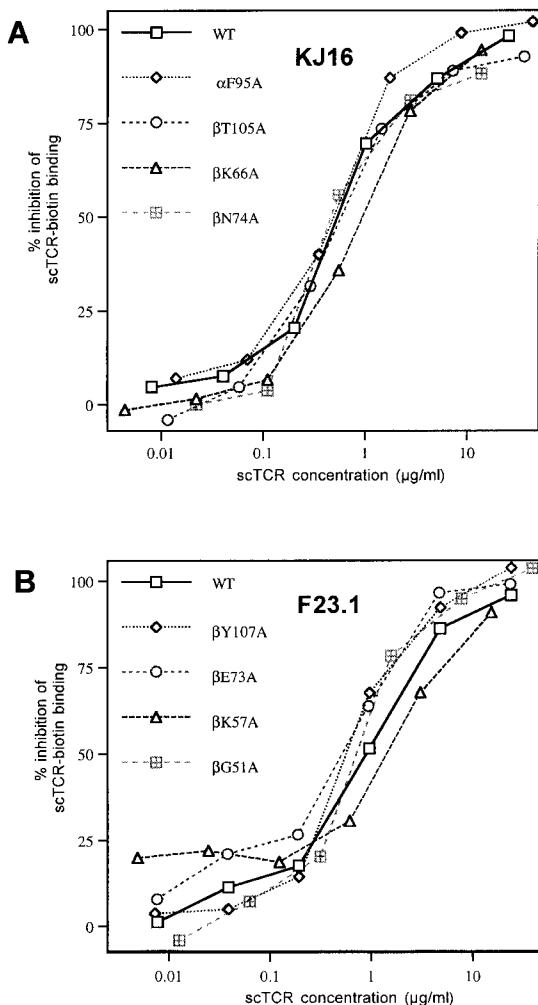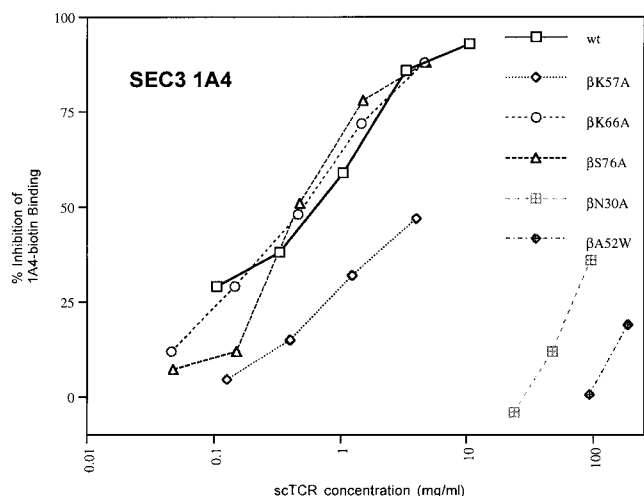
Figure 4. Competition ELISA of scTCR alanine mutants with SEC3-1A4. Inhibition of SEC3-1A4 binding by representative 2C scTCR alanine mutants. Wt and mutant scTCRs at various concentrations were used to inhibit the binding of biotinylated SAG SEC3-1A4 to wt-scTCR in an ELISA format. Bound biotinylated 1A4 was detected by streptavidin-HRP. The reactivity of each mutant was determined as the ratio of mutant to wt IC_{50} by linear regression analysis.

to wt-scTCR. The average value of three or more independent assays was used to determine binding affinities, relative to wt-scTCR (Fig. 5). In the other assay, BIAcore analyses were performed with immobilized SEC3-1A4. Various concentrations of mutant scTCRs were allowed to reach binding equilibrium, and the K_D of each mutant relative to wt-scTCR was determined by Scatchard analysis (43; Fig. 6). The values determined by the competition ELISA and SPR were completely consistent (Table I). Only the reactivity values determined from the competition assay are summarized as the bar graph in Fig. 5.

Many alanine scanning studies have shown that only a few mutations at a subset of the contact residues result in large (>10-fold) reductions in binding. In the TCR scan, only 6 of the 25 TCR residues tested affected the binding of SEC3-1A4 by >10-fold (Fig. 5). These six residues were distributed among CDR1 (28βAsn, 30βAsn), CDR2 (51βGly, 52βAla, 52βGly), and HV4 (72βGln). Residues with significant yet more limited effects were also present in each of these loops and in the FR3 region (57βLys). Consistent with previous predictions that SAGs are largely Vβ specific, neither the βCDR3 loop nor the most prominent residue (100αPhe) at the surface of the pMHC binding site contributed binding energy to the SEC3–TCR interaction.

Although the most important residues shown in Fig. 5 are distributed throughout the linear sequence, the energy map of these residues in the three dimensional structure re-
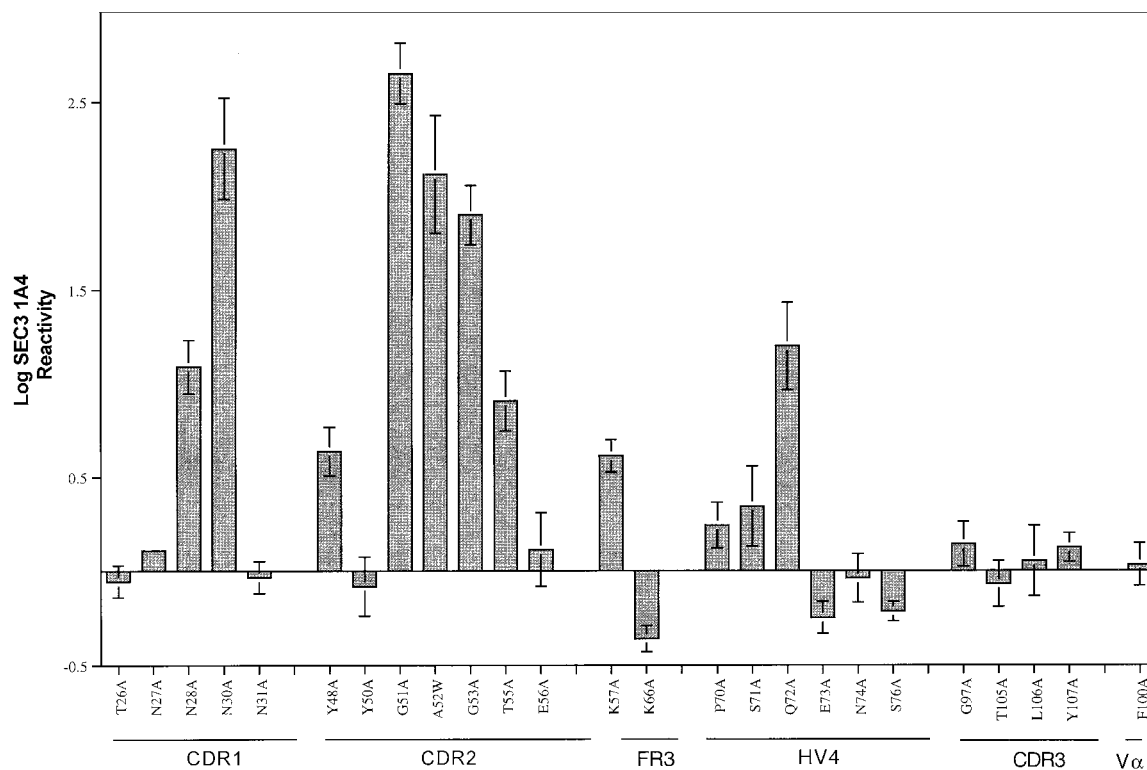

Figure 5. Reactivities of scTCR alanine mutants with SEC3-1A4. Reactivities of mutant proteins were determined as IC_{50} values relative to wt by linear regression analysis. Positive values (above the wt reference line of 0 reactivity) indicate a decrease in binding, and negative values indicate an increase in binding. Error bars represent three or more independent experiments.
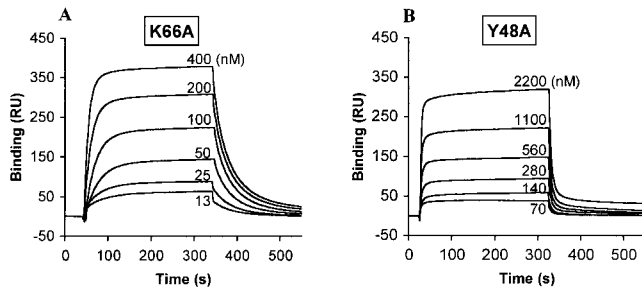
Figure 6. Sensorgrams of 2C TCR alanine mutants binding SEC3 variant 1A4. βK66A (A) and βY48A (B) were injected at the indicated concentrations at a flow rate of 15 μl/min over a surface to which SEC3-1A4 (500 RU) had been immobilized.

veals an energetic hotspot centered around CDR2 residues 51–53 (Fig. 7). This hotspot is surrounded by residues in CDR1, HV4, and FR3 that contribute to the binding interaction. With the exception of CDR1, each of these regions has residues that are in contact with wt SEC3 in the 14.3.d Vβ–SEC3 complex. Analysis of the interface of the Vβ–SEC3 complex (Fig. 8) suggests that the important residues in CDR1 (28βAsn, 30βAsn) and HV4 residue 72βGln exert their effects by interacting with the region of SEC3 that has been altered in the 1A4 variant (shown in red on the small domain of SEC3). Accordingly, the binding energies measured for CDR1 residues 28βAsn and 30βAsn are likely contributing to the higher affinity associated with the Vβ8–SEC3-1A4 interaction. The energy associated with these three residues (ΔΔG ∼ 4.8 Kcal/mol) in the alanine scan could account for the 200–300-fold increase in affinity of the SEC3-1A4 variant. We expect that a structure of the mutant SEC3–TCR complex could help substantiate this prediction, but for the purpose of examining the wt SEC3–Vβ interaction, CDR1 residues 28βAsn and 30βAsn and HV4 residue 72βGln will not be considered further.

The CDR2 region of the Vβ domain of the TCR has the majority of structural contacts in the complex with SEC3 (15, 16). Residues 52βAla and 53βGly contact SEC3 residues 90Tyr and 210Gln, respectively, two residues that were previously identified as TCR-binding "hotspots" within SEC3 (Fig. 8; reference 17). The most significant reduction in binding was observed for residue 51βGly, which also contacts SEC3 but does not contact SEB (16). Accordingly, this position may in part account for the higher affinity of Vβ8.2 for SEC3 compared with SEB. Although the two adjacent CDR2 residues 50βTyr and 56βGlu contact SEC3 residues 91Val and 20Thr, respectively, mutation of these residues did not show significant effects on binding. Thus, like other protein–protein interactions, the energetic hotspot of the SEC3–Vβ8 interaction does not extend across the entire interface. Vβ residue 48Tyr, which is distal to the Vβ–SEC3 interface (Fig. 8), results in a moderate loss of binding when changed to alanine, probably because of effects this mutation has on the local conformation of the CDR2 loop and possibly on FR3 residue 57βLys. Unfortu-

Table I. *Binding Energetics of 2C scTCR Alanine-substituted Mutants*

CDR loop	TCR residue	SEC3 structural contacts*	Hydrogen bond	ΔΔG‡	K_D BIAcore§
				kcal/mol ± SD	nM
CDR1β	T26	–	–	−0.07 ± 0.10	–
	N27	–	–	0.14 ± 0.03	–
	N28	S–S loop	–	1.36 ± 0.18	–
	N30	S–S loop	–	>2.12 ± 0.34	>1,200
	N31	–	–	−0.04 ± 0.11	–
CDR2β	Y48	–	–	0.80 ± 0.16	880
	Y50	V91	–	−0.10 ± 0.20	160
	G51	V91	–	>2.12 ± 0.20	>5,000
	A52	Y90	–	>2.12 ± 0.39	>5,000
	G53	N23, Y26, Q210	Q210	>2.12 ± 0.20	>5,000
	S54	N23, V91	–	–	–
	T55	T20, T20, N23	N23(2)	1.13 ± 0.20	–
	E56	T20	–	0.14 ± 0.24	–
FR3β	K57	G19, T20	–	0.77 ± 0.11	1,400
	K66	F176	–	−0.45 ± 0.09	120
	A67	F176	–	–	–
HV4β	P70	L58	N60	0.30 ± 0.15	–
	S71	N60	–	0.43 ± 0.27	–
	Q72	S–S loop	–	1.50 ± 0.29	–
	E73	–	–	−0.31 ± 0.10	–
	N74	–	–	−0.05 ± 0.16	200
	S76	–	–	−0.27 ± 0.06	–
CDR3β	G97	–	–	0.18 ± 0.15	400
	T105	–	–	−0.09 ± 0.15	–
	L106	–	–	0.07 ± 0.23	–
	Y107	–	–	0.16 ± 0.09	–
CDR3α	F100	–	–	0.04 ± 0.14	220

*Contact residues and hydrogen bonding data are from the SEC3–14.3.e β chain complex (references 15, 16; Protein Data Bank [available at http:\\www.rcsb.org/pdb] accession no. 1JCK.
‡Changes in free energy of binding were calculated from ELISA experiments based on IC$_{50}$ binding data relative to wt 2C scTCR. A maximum value of 2.1 kcal/mol corresponds to a 50-fold decrease in binding.
§Dissociation constants were determined by BIAcore experiments. The K_D of wt 2C scTCR–SEC3-1A4 complex is 185 nM.

nately, the contribution of 54βSer, which contacts SEC3 residues 23Asn and 91Val, could not be determined since this alanine mutant failed to refold correctly.

In comparison to CDR2, the more limited influence of HV4 residues on the SEC3 binding energy was consistent with the observation that the HV4 loop possesses fewer contacts in the 14.3.d β chain–SEC3 complex than the CDR2 loop (16). Vβ residues 70βPro and 71βSer, which
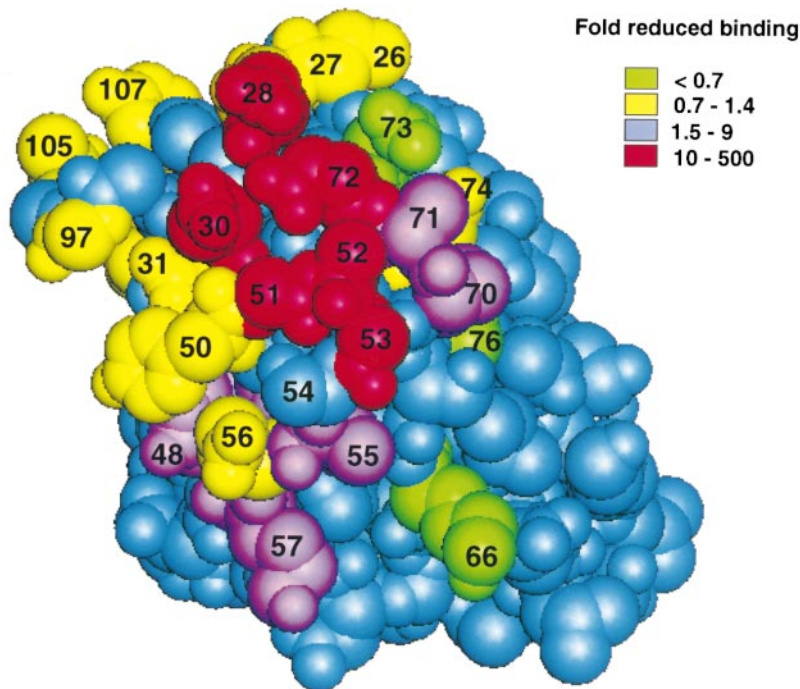
Figure 7. Energy map of the 2C scTCR SEC3-1A4 binding site. The face of the TCR Vβ domain that recognizes SEC3 is shown. The color scale indicates the fold reduction in binding for each residue upon alanine substitution (or tryptophan substitution of 52βAla): red shows a >10-fold reduction in binding, purple shows a 1.5–9-fold reduction in binding, yellow shows no effect on binding, and green shows an increase in binding. 106βLeu (yellow) is not shown. 54βSer was unable to be tested, as the alanine mutant lacked Vβ8-specific mAb activity. The 2C TCR surface illustrated is from the 2C TCR crystal structure (reference 35; Protein Data Bank [available at http:\\www.rcsb.org/pdb] accession no. 1TCR).

are on the proximal side of the HV4 loop and in contact with SEC3 residues 58Leu and 60Ser, contributed a moderate amount of binding energy. Mutation of residues on the distal side of the loop (73βGlu, 74βAsn, and 76βSer) did not reduce SEC3 binding and in fact alanine mutants of residues 73βGlu and 76βSer showed moderate increases in binding (see below). Residue 74βAsn is a possible glycosylation site in the native TCR. The observation that mutation of this position had no effect on SEC3 binding is consistent with previous findings that glycosylation of the TCR does not appear to affect SEC3 binding (43).

The two most accessible residues in Vβ FR3, 57βLys and 66βLys, are both in contact with SEC3 in the crystal structure. Mutation of 57βLys led to a moderate reduction in binding, probably due to the loss of multiple Van der Waals (vdw) interactions with SEC3 residues 19Gly and 20Thr. In contrast, alanine substitution of 66βLys led to a significant enhancement of binding (see below).

There were no direct contacts between CDR3 of 14.3.d TCR β chain and SEC3 observed in the crystal structure of the complex (15). Consistent with this finding, mutations at residues 97βGly, 105βThr, 106βLeu, and 107βTyr showed minimal effects on SEC3 binding. A small but consistent reduction in binding of the Gly97Ala mutation was observed in both the ELISA format (decrease of 1.4-fold) and by SPR ($K_D = 400$ nM). This result may suggest that the CDR3 loop is in a position to effect in a moderate way the binding of this SAG. As indicated above, Vα residue 100αPhe is the most prominent residue on the pMHC-binding surface (35), yet it had no effect on binding SEC3. A recent study has shown that Vα CDR2 residues can affect binding to the SEC3–MHC complex but not to SEC3 alone (18).

Enhanced Binding of TCR Mutants to SEC3. Most alanine

scanning studies reveal a fraction of mutations that lead to slight increases in the binding of ligand (44). In the case of the TCR–SEC3 interaction, mutations at three TCR residues (66βLys, 73βGlu, and 76βSer) showed minor but significant increases in binding (Fig. 5). To determine if the combination of these mutations would yield further increases in affinity, all three residues were examined as double and triple mutants (Fig. 9). Each of the three double mutants exhibited affinities for the SEC3 that were above the single-site mutants. The triple mutant yielded the highest affinity, approximately fivefold greater than the wt-scTCR. The mechanism by which these modified side chains act to increase the affinity is unknown, but presumably the alanine mutations could: (a) eliminate steric interferences of the wt side chain, (b) stabilize the TCR in a conformation that recognizes the ligand, or (c) allow increased mobility of TCR regions that require such flexibility in the recognition of ligands. Our recent analyses of several TCR mutants that bind pMHC with higher affinity suggest that each of these possibilities might operate, depending on the residue, its location in the structure, and the ligand itself (45; and Lee, P.U.Y., H.R.O. Churchill, and D.M. Krantz, unpublished findings).

Discussion

Alanine scanning mutagenesis has been used to characterize the functional contribution of individual residues in several protein–protein interactions, including antigen–antibody interactions (27, 46) and TCR–SEC3 (17). Since alanine substitution minimizes steric and/or electrostatic constraints on the tertiary structure of a protein, this approach provides a systematic analysis of protein binding
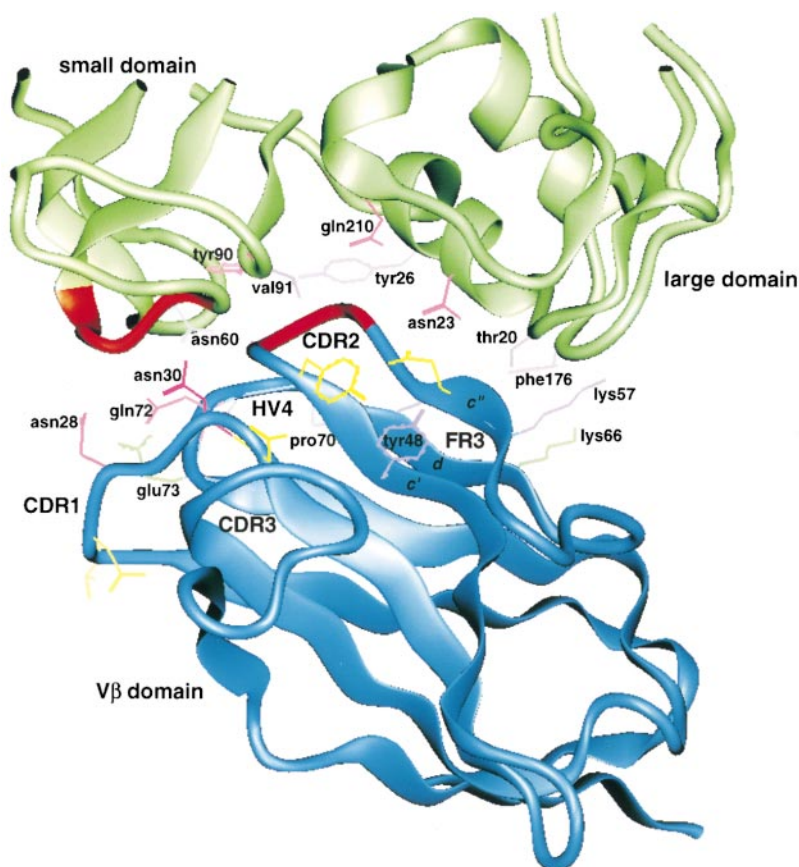
Figure 8. Binding interface of the Vβ8 domain and SEC3. The binding interface of the TCR Vβ8 (blue) and SEC3 (green) is shown. Residues that were subjected to alanine scanning in the TCR and SEC3 (reference 17) are shown. The color scale indicates the fold reduction in binding for each residue: red shows the greatest reduction in binding, purple shows a moderate effect, yellow shows little effect, and green shows an increase in binding. The SEC3 loop colored red indicates the affinity maturation site of the SEC3-A4 variant. The region of CDR2β colored red (51βGly, 52βAla, 53βGly) contributed the greatest energy to the interaction. A view of the CDR2β loop of the TCR shows the topology of the *c″* β strand in relation to the *c′* and *d* strands. Coordinates are derived from the 14.3.d TCR–SEC3 crystal structure (reference 15; Brookhaven Protein Data Bank accession no. 1JCK).
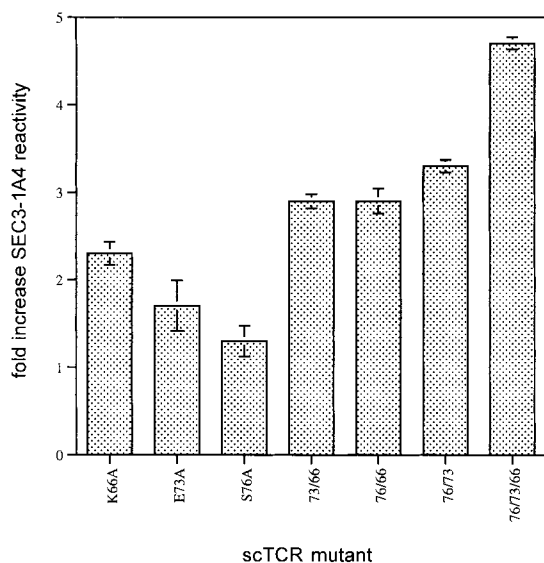

Figure 9. Reactivities of double and triple scTCR alanine mutants with SEC3-1A4. Fold increases of SEC3-1A4 reactivity were calculated based on the relative IC_{50} of each mutant compared with wi using linear regression analysis. Error bars represent the SD obtained from three separate ELISA experiments.

thermodynamics (26, 44). In this report, the relative contributions of Vβ residues in binding SEC3 were examined by alanine scanning mutagenesis. From these results, the energy of the TCR interface with SEC3 can be mapped as the change in binding free energy (ΔΔG) for each mutation (Table I, and Fig. 5). The CDR2, CDR1, HV4, FR3, and CDR3 regions accounted for 59, 25, 11, 2, and 2%, respectively, of the 2C TCR binding energy toward the SEC3 variant 1A4. The mutated region of SEC3 in 1A4 is within the disulfide loop. This loop is believed to be highly flexible based on its poor resolution in crystal structures, even at 1.5 Å resolution (47). Least square superpositioning of structures of SEC3 and SEC3 in complex with the 14.3.d TCR β chain suggested that the loop could be very close to residues within the Vβ8 CDR1 and to HV4 residue 72βGln. Thus, we suspect that these residues affected binding to 1A4 because they are involved in contacts with the mutated SEC3 region.

With this in mind, the thermodynamic results shown here point to the significant energetic contribution of the CDR2 loop in SEC3 recognition by Vβ8.2 and they define this region as the hotspot of the TCR–SEC3 interaction. This hotspot is located at the tip of CDR2, and it involves predominantly residues 51βGly, 52βAla, and 53βGly. These are surrounded by a second shell of residues that appear to contribute a moderate amount of energy to the interaction: 55βThr, 57βLys, 70βPro, and 71βSer. Residue 54βSer is located within the same region but it

was unable to be tested because the alanine mutant did not fold properly. The results are also consistent with the alanine scan that was performed from the SEC3 side of the interaction, in that most of the key residues in SEC3 are located within proximity to the key residues in the Vβ domain (Fig. 8; reference 17). It is important to point out that the exact energetic contributions of side chains within the CDR2 loop cannot be determined from this analysis. This is because analysis of the wt residues 51βGly, 52βAla, and 53βGly necessitated mutation to larger groups at the interface (51βAla, 52βTrp, and 53βAla, respectively), and these modifications may act by interfering with main chain interactions. Nevertheless, even more extensive changes are seen among other Vβ regions that are SEC3 reactive (Table II; reference 3), suggesting that there are significant compensatory interactions that occur at TCR–SEC3–MHC interfaces (see below).

Direct comparison of the structures of the Vβ8.2 domain of the 14.3.d TCR and the corresponding domains of several other TCRs suggested a possible explanation for the Vβ-related specificity of SEC3 and SEB (12, 16). The 14.3.d Vβ8.2 region and the SEC3-reactive human Vβ12.3 from the A6 TCR (48) showed an root mean squared (rms) difference of 0.9 Å when the 14 α-carbon atoms in the SEC3/SEB-binding site were superimposed. In contrast, the 14.3.d Vβ8.2 region and the SEC3-nonreactive mouse Vβ2.3 from the KB5-C20 TCR (49) showed an r.m.s difference of 3.0 Å for the same 14 α-carbon atoms in the SEC3/SEB-binding site. This significant difference in alignment is due primarily to the c'' β strand hydrogen bonding to the outer β sheet d strand in Vβ2.3, instead of maintaining association with the c' strand of its inner β sheet, as is the case with Vβ8.2 and Vβ12.3 (16, 49). The altered orientation of the c'' strand in relation to the c' and d strands directly affects the conformations of CDR2 and FR3 (Fig. 8). Therefore, the spatial integrity of the c'' strand in relation to the c' and d strands appears to impose a conformational restriction that is important for the binding motif of SEB and SEC3. This implies that other Vβ subsets that bind these SAGs may show c'' conformational similarity to mouse Vβ8 and human Vβ12.

Several of the mutations that affected SEC3 binding appear to act by disrupting this conserved topology within the c'' and d strand interactions. For example, 48βTyr interacts with 55βThr and 56βGlu on the c'' strand. The side chain of 55βThr on the c'' strand is hydrogen-bonded to its own main chain oxygen and involved in multiple vdw interactions with 69βArg on the d strand. This mutation could thereby disrupt hydrogen bonds that the c' strand shares with SEC3 residues 20Thr and 23Asn.

The results shown here also provide a rationale for the importance of CDR2 residues 51–53 in the interactions of Vβ regions with SEC3 and SEB. Multiple hydrogen bonds and vdw interactions are formed with these Vβ8.2 residues and the conserved SAG residues 23Asn, 60Asn, and 90Tyr (16). However, the affinity of the Vβ8.2 region for SEB has been reported to be 100-fold less than for SEC3. Glyβ53 has 1 contact with SEB residue 23Asn but 11 addi-

Table II. *Sequences of Mouse and Human Vβ Regions That Are SEC3 Reactive*

Vβ family	50	51	52	53	54	55	56	57	66	70	71
mVβ8.2	Y	G	A	G	S	T	E	K	K	P	S
Effect of mutation:		***	***	***		**		**		**	**
mVβ3	Q	N	Q	E	V	L	Q	Q	S	P	S
mVβ7	Y	D	V	D	S	N	S	E	R	K	K
mVβ10	N	N	K	Q	L	I	V	N	S	S	S
mVβ17	R	N	E	E	I	M	E	Q	S	S	S
hVβ3	Y	D	V	K	M	K	E	K	S	E	K
hVβ5	F	S	E	T	Q	R	N	K	S	F	S
hVβ12	Y	G	V	K	D	T	D	K	S	S	K
hVβ13.2	V	G	E	G	T	T	A	K	N	L	K
hVβ14	M	N	V	E	V	T	D	K	K	K	E
hVβ15	F	D	V	K	D	I	N	K	S	Q	A
hVβ17	Q	I	V	N	D	F	Q	K	S	E	K
hVβ20	V	G	I	G	Q	I	S	S	S	P	Q

Amino acid residues that are present at positions near the Vβ8–SEC3 interface are shown for various mouse (mVβ) and human (hVβ) TCRs (reference 3). Effects of mutations on SEC3 binding by the Vβ8.2 region are shown as ***>10-fold reduction in binding or as **1.5–9-fold reduction in binding. All of the Vβ8.2 residues shown were examined in the present mutational analysis, except Serβ54Ala, which was defective in folding.

tional vdw interactions with SEC3 residues 26Tyr and 210Gln. Since this position in CDR2 is a hotspot of SEC3 binding ($\Delta\Delta G > 2$ kcal/mol), loss of these multiple contacts in the SEB complex may account for its lower affinity for the TCR compared with SEC3. Consistent with this possibility, mutation of SEB 26Val, which does not contact 53βGly, to the SEC3 residue tyrosine resulted in a higher affinity for the SEB/26Tyr variant ($K_D \sim 12$ μM; reference 17). Similarly, 51βGly has four contacts with SEC3 residue 91Val, but does not contact SEB residue 91Tyr.

Perhaps the most unexpected finding of the current study is that there were significant effects of many single-site mutations that are at the interface, but which lack direct side chain interactions with the wt SEC3 in the structure. In this regard, 57βLys is the only residue that exhibits side chain hydrogen bonds that contact SEC3. Other residues exhibit hydrogen bonds between main chain atoms and SEC3. One might expect these interactions to be largely sequence independent, consistent with the extensive diversity present among SEC3-reactive Vβ regions in the residues at the interface. With this in mind, it is reasonable to ask how do alanine substitutions reduce binding by up to 100-fold (e.g., Gly51βAla and Gly53βAla), if the primary interactions involve hydrogen bonds between SEC3 and Vβ main chain atoms? We consider two general features of a Vβ region that may be necessary (although not sufficient) for productive binding to SEC3. First, as previously discussed, the overall topology of the Vβ domain

must conform to that observed in the crystal structures of the SEC3-reactive Vβ domains (12). Second, even with this scaffold, the conformations of CDR2 and HV4 loops can be affected by single residues, thereby impacting specific main chain interactions with SEC3. These effects on conformation might involve loop dynamics and mobility without altering the major backbone conformation observed in the crystal structures. A recent solution structure of an scTCR observed such mobility, but primarily in the CDR3 loops (50). Conformational plasticity was also observed in the interaction of the 2C TCR with the pMHC complex dEV8/K^b, but the major structural changes were in CDR3α and, to a lesser extent, CDR1α (51). In addition, studies of single-site variants in antigen–antibody interactions have shown that there can be entropic compensation for losses of enthalpy (52).

If single-site mutations observed in this report can so significantly affect SEC3 binding, then how do other SEC3-reactive Vβ regions, which have extensive diversity in this same set of residues (Table II), maintain SEC3 reactivity? Although the answer to this question will come from detailed structural and mutagenic analyses of these Vβ regions, it is important to note that the binding affinities of SEC3 for most of the different Vβ regions have not been measured (12). It is possible that the variability found at key Vβ positions will confer upon these Vβ regions a range of affinities for SEC3, some of which differ significantly from that measured for the Vβ8.2 region. Thus, these interactions could exhibit a range of affinities that is as large as the difference between the affinities measured for Vβ8.2 interacting with SEB and with SEC3 (∼140-fold). From the functional perspective, this is not an unreasonable possibility, as it is clear that a 100-fold lower affinity of the TCR–SAG interaction may only affect the biological activity moderately, whereas the SAG–MHC affinity has a greater effect on function (17, 53). As the Vα region is now thought to participate directly in the interaction with class II MHC (at least in some cases), it is also possible that some Vβ–SEC3 interactions are below the measurable affinity range, yet the entire VαVβ–SEC3–class II complexes are sufficiently stable to elicit T cell activity. In this model, the requirement for Vα–class II interaction (and perhaps CDR3 involvement) then depends on some basal affinity of the Vβ–SAG interaction. This possibility could be tested by measuring the affinities of the different Vβ regions for SEC3 and examining the restrictions in Vα use (focusing on CDR2α in particular) among T cells bearing the corresponding Vβ region. The latter approaches have already been taken for several SAGs, demonstrating that some appear to require either CDR3 or Vα interactions (8, 19–25).

The observation that single amino acid differences in the area of contact can reduce the binding energy by >10-fold also provides an explanation for the diverse biological effects of the same SAG. Previous binding studies with TCR–pMHC have shown that there is as little as a three-fold difference in affinities between agonist and antagonist responses (28, 29). It is apparent that minor differences in

Vβ sequence, or residues in CDR3β or the Vα region could either reduce or enhance the basal affinity of the Vβ–SAG–MHC interactions. The range of outcomes could be T cells that undergo full activation to T cells that undergo anergy.

We have also shown here that it is possible to increase the affinity of the TCR for SEC3 by approximately five-fold through the selected combination of alanine mutations. Although a fivefold increase is not likely to be sufficient for using soluble versions of the TCR as SEC3 antagonists, it does provide a guide for further engineering of high-affinity TCR by focusing on these residues. Furthermore, the findings suggest that other Vβ regions could have evolved compensatory mutations that act by increasing the affinities of the TCR for SAGs to some threshold level. A study of the human growth hormone receptor showed that analogous compensatory mutations at the hormone interface acted through local structural rearrangements in the region of contact (54). Some of these changes affected residues at 15 Å distance from the mutation. Likewise, the interactions of mutants of D5.1 antilysozyme and lysozyme have shown that altered residues can compensate, even at long distances, through reorganization of solvent at the interface (52, 55). It is reasonable to think that the other Vβ regions will likewise have local structural rearrangements at the SEC3 interface in order to achieve the minimal affinity necessary (K_D ∼100 μM) for stimulating T cells. The fact that multiple solutions to this interaction might have evolved among Vβ regions with the same scaffold suggests that there was strong selective pressure on SAGs to maintain binding to these diverse T cells.

References

1. Marrack, P., and J. Kappler. 1990. The staphylococcal enterotoxins and their relatives. *Science.* 248:705–711.
2. Papageorgiou, A.C., and K.R. Acharya. 1997. Superantigens as immunomodulators: recent structural insights. *Structure.* 5:991–996.
3. Kotzin, B.L., D.Y.M. Leung, J. Kappler, and P. Marrack. 1993. Superantigens and their potential role in human disease. *Adv. Immunol.* 54:99–166.
4. Scherer, M.T., L. Ignatowicz, G.M. Winslow, J.W. Kappler, and P. Marrack. 1993. Superantigens: bacterial and viral proteins that manipulate the immune system. *Annu. Rev. Cell Biol.* 9:101–128.

5. Bernal, A., T. Proft, J.D. Fraser, and D.N. Posnett. 1999. Superantigens in human disease. *J. Clin. Immunol.* 19:149–157.

6. Lavoie, P.M., J. Thibodeau, F. Erard, and R.P. Sekaly. 1999. Understanding the mechanism of action of bacterial superantigens from a decade of research. *Immunol. Rev.* 168:257–269.

7. Cole, B.C., and M.M. Griffiths. 1993. Triggering and exacerbation of autoimmune arthritis by the *Mycoplasma arthritidis* superantigen MAM. *Arthritis Rheum.* 36:994–1002.

8. Hodtsev, A.S., Y. Choi, E. Spanopoulou, and D.N. Posnett. 1998. Mycoplasma superantigen is a CDR3-dependent ligand for the T cell antigen receptor. *J. Exp. Med.* 187:319–327.

9. Bohach, G.A., D.J. Fast, R.D. Nelson, and P.M. Schlievert. 1990. Staphylococcal and streptococcal pyrogenic toxins involved in toxic shock syndrome and related illnesses. *Crit. Rev. Microbiol.* 17:251–272.

10. Li, P.L., R.E. Tiedemann, S.L. Moffatt, and J.D. Fraser. 1997. The superantigen streptococcal pyrogenic exotoxin C (SPE-C) exhibits a novel mode of action. *J. Exp. Med.* 186:375–383.

11. Proft, T., S.L. Moffatt, C.J. Berkahn, and J.D. Fraser. 1999. Identification and characterization of novel superantigens from *Streptococcus pyogenes. J. Exp. Med.* 189:89–102.

12. Li, H., A. Llera, E.L. Malchiodi, and R.A. Mariuzza. 1999. The structural basis of T cell activation by superantigens. *Annu. Rev. Immunol.* 17:435–466.

13. Choi, Y., A. Herman, D. DiGusto, T. Wade, P. Marrack, and J. Kappler. 1990. Residues of the variable region of the T cell receptor β chain that interact with *S. aureus* toxin superantigens. *Nature.* 346:471–473.

14. Patten, P.A., E.P. Rock, T. Sonoda, B.F. de St. Groth, J.L. Jorgensen, and M.M. Davis. 1993. Transfer of putative complementarity-determining region loops of T cell receptor V domains confers toxin reactivity but not peptide/MHC specificity. *J. Immunol.* 150:2281–2294.

15. Fields, B.A., E.L. Malchiodi, H. Li, X. Ysern, C.V. Stauffacher, P.M. Schlievert, K. Karjalainen, and R.A. Mariuzza. 1996. Crystal structure of a T-cell receptor β-chain complexed with a superantigen. *Nature.* 384:188–192.

16. Li, H., A. Llera, D. Tsuchiya, L. Leder, X. Ysern, P.M. Schlievert, K. Karjalainen, and R.A. Mariuzza. 1998. Three-dimensional structure of the complex between a T cell receptor beta chain and the superantigen staphylococcal enterotoxin B. *Immunity.* 9:807–816.

17. Leder, L., A. Llera, P.M. Lavoie, M.I. Lebedeva, H. Li, R.P. Sekaly, G.A. Bohach, P.J. Gahr, P.M. Schlievert, K. Karjalainen, and R.A. Mariuzza. 1998. A mutational analysis of the binding of staphylococcal enterotoxins B and C3 to the T cell receptor beta chain and major histocompatibility complex class II. *J. Exp. Med.* 187:823–833.

18. Andersen, P.S., P.M. Lavoie, R.P. Sekaly, H. Churchill, D.M. Kranz, P.M. Schlievert, K. Karjalainen, and R.A. Mariuzza. 1999. Role of the T cell receptor alpha chain in stabilizing TCR-superantigen-MHC class II complexes. *Immunity.* 10:473–483.

19. Smith, H.P., P. Le, D.L. Woodland, and M.A. Blackman. 1992. T cell receptor alpha-chain influences reactivity to Mls-1 in V beta 8.1 transgenic mice. *J. Immunol.* 149:887–896.

20. Woodland, D.L., H.P. Smith, S. Surman, P. Le, R. Wen, and M.A. Blackman. 1993. Major histocompatibility complex–specific recognition of Mls-1 is mediated by multiple elements of the T cell receptor. *J. Exp. Med.* 177:433–442.

21. Surman, S., A.M. Deckhut, M.A. Blackman, and D.L. Woodland. 1994. MHC-specific recognition of a bacterial superantigen by weakly reactive T cells. *J. Immunol.* 152:4893–4902.

22. Daly, K., P. Nguyen, D. Hankley, W.J. Zhang, D.L. Woodland, and M.A. Blackman. 1995. Contribution of the TCR α-chain to the differential recognition of bacterial and retroviral superantigens. *J. Immunol.* 155:27–34.

23. Liao, L., A. Marinescu, A. Molano, C. Ciurli, R.P. Sekaly, J.D. Fraser, A. Popowicz, and D.N. Posnett. 1996. TCR binding differs for a bacterial superantigen (SEE) and a viral superantigen (Mtv-9). *J. Exp. Med.* 184:1471–1482.

24. Bravo de Alba, Y., P.N. Marche, P.A. Cazenave, I. Cloutier, R.P. Sekaly, and J. Thibodeau. 1997. V alpha domain modulates the multiple topologies of mouse T cell receptor V beta20/staphylococcal enterotoxins A and E complexes. *Eur. J. Immunol.* 27:92–99.

25. Ciurli, C., D.N. Posnett, R.P. Sekaly, and F. Denis. 1998. Highly biased CDR3 usage in restricted sets of beta chain variable regions during viral superantigen 9 response. *J. Exp. Med.* 187:253–258.

26. Wells, J. 1991. Systematic mutational analyses of protein-protein interfaces. *Methods Enzymol.* 202:390–411.

27. Dall'Acqua, W., E.R. Goldman, E. Eisenstein, and R.A. Mariuzza. 1996. A mutational analysis of the binding of two different proteins to the same antibody. *Biochemistry.* 35:9667–9676.

28. Alam, S.M., P.J. Travers, J.L. Wung, W. Nasholds, S. Redpath, S.C. Jameson, and R.J. Gascoigne. 1996. T cell receptor affinity and thymocyte positive selection. *Nature.* 381:616–620.

29. Manning, T.C., and D.M. Kranz. 1999. Binding energetics of T-cell receptors: correlation with immunological consequences. *Immunol. Today.* 20:417–422.

30. Landt, O., H. Grunert, and U. Hahn. 1990. A general method for rapid site-directed mutagenesis using the polymerase chain reaction. *Gene.* 96:125–128.

31. Schodin, B.A., C.J. Schlueter, and D.M. Kranz. 1996. Binding properties and solubility of single-chain T cell receptors expressed in *E. coli. Mol. Immunol.* 33:819–829.

32. Haskins, K., C. Hannum, J. White, N. Rhoem, R. Kubo, J. Kappler, and K. Marrack. 1984. The antigen-specific major histocompatibility complex–restricted receptor on T cells. VI. An antibody to a receptor allotype. *J. Exp. Med.* 160:452–471.

33. Staerz, U.D., H.G. Rammensee, J.D. Benedetto, and M.J. Bevan. 1985. Characterization of a murine monoclonal antibody specific for an allotypic determinant on T cell antigen receptor. *J. Immunol.* 134:3994–4000.

34. Schuck, P., P.S. Andersen, and L. Boyd. 1999. Measuring protein interactions using optical biosensors. *Curr. Protocols Protein Sci.* 2:20.2.1–20.2.21.

35. Garcia, K.C., M. Degano, R.L. Stanfield, A. Brunmark, M.R. Jackson, P.A. Peterson, L. Teyton, and I.A. Wilson. 1996. An αβ T cell receptor structure at 2.5 Å and its orientation in the TCR-MHC complex. *Science.* 274:209–219.

36. Kranz, D.M., D.H. Sherman, M.V. Sitkovsky, M.S. Pasternack, and H.N. Eisen. 1984. Immunoprecipitation of cell surface structure of cloned cytotoxic T lymphocytes by clone-specific antisera. *Proc. Natl. Acad. Sci. USA.* 81:573–577.

37. Udaka, K., T.J. Tsomides, and H.N. Eisen. 1992. A naturally occurring peptide recognized by alloreactive CD8+ cytotoxic T lymphocytes in association with a class I MHC protein. *Cell.* 69:989–998.

38. Sha, W.C., C.A. Nelson, R.D. Newberry, J.K. Pullen, L.R. Pease, J.H. Russell, and D.Y. Loh. 1990. Positive selection of transgenic receptor-bearing thymocytes by Kb antigen is altered by Kb mutations that involve peptide binding. *Proc. Natl. Acad. Sci. USA.* 87:6186–6191.

39. Schlueter, C.J., B.A. Schodin, S.Y. Tetin, and D.M. Kranz. 1996. Specificity and binding properties of a single-chain T cell receptor. *J. Mol. Biol.* 256:859–869.

40. Schlueter, C.J., T.C. Manning, B.A. Schodin, and D.M. Kranz. 1996. A residue in the center of peptide QL9 affects binding to both L^d and the T cell receptor. *J. Immunol.* 157: 4478–4485.

41. Brodnicki, T.C., P.O. Holman, and D.M. Kranz. 1996. Reactivity and epitope mapping of single-chain T cell receptors with monoclonal antibodies. *Mol. Immunol.* 33:253–263.

42. Manning, T.C., C.J. Schlueter, T.C. Brodnicki, E.A. Parke, J.A. Speir, K.C. Garcia, L. Teyton, I.A. Wilson, and D.M. Kranz. 1998. Alanine scanning mutagenesis of an αβ T cell receptor: mapping the energy of antigen recognition. *Immunity.* 8:413–425.

43. Malchiodi, E.L., E. Eisenstein, B.A. Fields, D.H. Ohlendorf, P.M. Schlievert, K. Karjalainen, and R.A. Mariuzza. 1995. Superantigen binding to a T cell receptor β chain of known three-dimensional structure. *J. Exp. Med.* 182:1833–1845.

44. Bogan, A.A., and K.S. Thorn. 1998. Anatomy of hot spots in protein interfaces. *J. Mol. Biol.* 280:1–9.

45. Manning, T.C., E.A. Parke, L. Teyton, and D.M. Kranz. 1999. Effects of complementarity determining region mutations on the affinity of an αβ T cell receptor: measuring the energy associated with CD4/CD8 repertoire skewing. *J. Exp. Med.* 189:461–470.

46. Jin, L., and J.A. Wells. 1994. Dissecting the energetics of an antibody-antigen interface by alanine shaving and molecular grafting. *Protein Sci.* 3:2351–2357.

47. Papageorgiou, A.C., H.S. Tranter, and K.R. Acharya. 1998. Crystal structure of microbial superantigen staphylococcal enterotoxin B at 1.5 Å resolution: implications for superantigen recognition by MHC class II molecules and T-cell receptors. *J. Mol. Biol.* 277:61–79.

48. Garboczi, D.N., P. Ghosh, U. Utz, Q.R. Fan, W.E. Biddison, and D.C. Wiley. 1996. Structure of the complex between human T-cell receptor, viral peptide and HLA-A2. *Nature.* 384:131–141.

49. Housset, D., G. Mazza, C. Gregoire, C. Piras, B. Malissen, and J.C. Fontecilla-Camps. 1997. The three dimensional structure of a T-cell antigen receptor VαVβ heterodimer reveals a novel arrangement of the Vβ domain. *EMBO (Eur. Mol. Biol. Organ.) J.* 16:4205–4216.

50. Hare, B.J., D.F. Wyss, M.S. Osburne, P.S. Kern, E.L. Reinherz, and G. Wagner. 1999. Structure, specificity and CDR mobility of a class II restricted single-chain T-cell receptor. *Nat. Struct. Biol.* 6:574–581.

51. Garcia, K.C., M. Degano, L.R. Pease, M. Huang, P. Peterson, L. Teyton, and I.A. Wilson. 1998. Structural basis of plasticity in T cell receptor recognition of a self peptide-MHC antigen. *Science.* 279:1166–1172.

52. Braden, B.C., E.R. Goldman, R.A. Mariuzza, and R.J. Poljak. 1998. Anatomy of an antibody molecule: structure, kinetics, thermodynamics and mutational studies of the antilysozyme antibody D1.3. *Immunol. Rev.* 163:45–57.

53. Proft, T., and J. Fraser. 1998. Superantigens: just like peptides only different. *J. Exp. Med.* 187:819–821.

54. Atwell, S., M. Ultsch, A.M. De Vos, and J.A. Wells. 1997. Structural plasticity in a remodeled protein-protein interface. *Science.* 278:1125–1128.

55. Goldman, E.R., W. Dall'Acqua, B.C. Braden, and R.A. Mariuzza. 1997. Analysis of binding interactions in an idiotope-antiidiotope protein-protein complex by double mutant cycles. *Biochemistry.* 36:49–56.